

Special Issue: SERS-TERS

Applied Spectroscopy

Applied Spectroscopy 2020, Vol. 74(11) 1374–1383 © The Author(s) 2020 Article reuse guidelines: sagepub.com/journals-permissions DOI: 10.1177/0003702820937333 journals.sagepub.com/home/asp



Capture of Phenylalanine and Phenylalanine-Terminated Peptides Using a Supramolecular Macrocycle for Surface-Enhanced Raman Scattering Detection

Jacob E. Olson¹, Adam S. Braegelman², Lei Zou², Matthew J. Webber², and Jon P. Camden¹

Abstract

The cucurbit[n]uril (CB[n]) family of macrocycles are known to bind a variety of small molecules with high affinity. These motifs thus have promise in an ever-growing list of trace detection methods. Surface-enhanced Raman scattering (SERS) detection schemes employing CB[n] motifs exhibit increased sensitivity due to selective concentration of the analyte at the nanoparticle surface, coupled with the ability of CB[n] to facilitate the formation of well-defined electromagnetic hot spots. Herein, we report a CB[7] SERS assay for quantification of phenylalanine (Phe) and further demonstrate its utility for detecting peptides with an N-terminal Phe. The CB[7]—guest interaction improves the sensitivity 5–25-fold over direct detection of Phe using citrate-capped silver nanoparticle aggregates, enabling use of a portable Raman system. We further illustrate detection of insulin via binding of CB[7] to the N-terminal Phe residue on its B-chain, suggesting a general strategy for detecting Phe-terminated peptides of clinically relevant biomolecules.

Keywords

Cucurbituril, amino acid, phenylketonuria, diabetes

Date received: 27 April 2020; accepted: I June 2020

Introduction

The amino acid L-phenylalanine (Phe) is prevalent in human metabolic pathways and is further hydroxylated into L-tyrosine (Tyr) by phenylalanine hydroxylase (PAH) for use in other metabolic pathways. Disruption of this process, such as a mutation in the PAH gene, leads to phenylketonuria (PKU) wherein PAH can no longer convert Phe into Tyr and Phe levels become elevated. This condition causes toxic levels of Phe to build up in the brain, leading to symptoms including declined cognitive ability, loss of motor function, and seizures.² To properly diagnose PKU, quantitative measurements of Phe are performed. Current standards for Phe detection include high-performance liquid chromatography (HPLC) coupled with mass spectrometry (MS) and HPLC coupled with fluorimetric detection via tagging. These methods, however, require expensive instrumentation and complicated sample modification. Further studies have explored aptamer-based techniques for Phe capture, but these rely on expensive surface ligands and do not provide a characteristic molecular spectrum. ^{4,5} Also these aptamer-based detection methods lack versatility, as they only detect Phe and have not been shown to detect larger peptides through their Phe-residues.

Insulin, which has an N-terminal Phe residue on its B-chain, is a peptide hormone integral in glucose regulation and metabolism with important implications in the diagnosis and treatment of diabetes. Various analytical methods

Corresponding Authors:

Matthew J. Webber, University of Notre Dame, 2058 McCourtney Hall, Notre Dame, IN 46556, USA.

Email: mwebber@nd.edu

Jon P. Camden, Department of Chemistry and Biochemistry, University of Notre Dame, I40E McCourtney Hall, Notre Dame, IN 46556, USA Email: jon.camden@nd.edu

¹Department of Chemistry and Biochemistry, University of Notre Dame, Notre Dame, USA

²Department of Chemical and Biomolecular Engineering, University of Notre Dame, Notre Dame, USA

for insulin detection have been studied including immuno-assays⁶ and MS;⁷ however, these techniques require expensive and bulky on-site instrumentation. Recent studies in optical detection methods have been based on surface plasmon resonance⁸ and fluorescence resonance energy transfer,⁹ but these methods rely on broad spectral signatures not specific to the molecular fingerprint of the analyte. Thus, there remains a need for inexpensive yet specific detection of insulin and related peptides which would leverage field-deployable instrumentation.

Surface-enhanced Raman scattering (SERS) is a robust analytical technique combining high-sensitivity and vibrational fingerprint analysis with the ability to use inexpensive, field-deployable instrumentation. 10 SERS-based methods rely on plasmon-supporting noble metal substrates to greatly enhance weak Raman signals;11 the greatest surface-enhancements are achieved when the molecule is adsorbed, or in very close proximity, to the nanoparticle (NP) surface. 12 Typically, compounds with surface-seeking functional groups are advantageous for SERS, as no further surface modification is needed, yet often analytes of interest lack such functional groups. A variety of methods are now employed to facilitate SERS detection of analytes with low surface affinity, including SERS-active tags and surface affinity strategies. 13-15 These techniques rely on mediating the interactions between the surface and the analyte via a capture ligand. SERS methods of Phe detection, however, have mainly relied on direct adsorption of Phe to a noble metal substrate with no surface ligand. 16,17 The use of a capture agent with Phe affinity should afford enhanced SERS sensitivity in detecting this analyte.

Cucurbit[n]urils (CB[n]s) are a family of macrocycles formed by acid-catalyzed condensation polymerization of n glycoluril monomers. 18 These and other macrocycles serve as host receptors in binding a variety of small molecule guests within the cavity of the macrocycle, with possible applications in affinity-mediated binding and sensing. [19,20] CB[n] has particular applicability in SERS techniques as its carbonyl-fringed portal offers affinity for noble metal surfaces, enabling the macrocycle to lay flat with its portal exposed; SERS enhancements of up to 109 are thus afforded through formation of NP hostspots.²¹ These enhancements give rise to SERS assays with detection capabilities down to 10^{-11} M, with even the single molecule regime possible.^{22,23} CB[n] increases SERS sensitivity through compound capture at the interface, with surface localization affording increased SERS sensitivity specifically in detecting molecules without surface-seeking functional groups. 21,24 Guest molecules with particularly strong affinity in binding to CB[n] macrocycles have a hydrophobic motif for inclusion in the cavity adjacent to a cationic motif to afford ion-dipole interactions with the electronegative carbonyl portal.²⁵ The CB[7] variant is particularly advantageous for SERS detection due to its high water solubility, an ability to encapsulate bulkier guest molecules, and

typically higher binding affinities relative to other CB[n] variants and related macrocycles. ^{26,27}

One interesting feature of CB[7] is its demonstrated high-affinity binding for Phe and related aromatic amino acids, with affinity (K_a) on the order of $10^5 \, \mathrm{M}^{-1}$ reported for CB[7] binding to Phe. 28 When this amino acid is presented on the N-terminus of a peptide or protein and the free carboxylate is replaced with an amide, binding is further increased by an order of magnitude or more.^{29,30} This feature of CB[7] affinity was shown to enable specific binding to the N-terminal Phe residue on the B-chain of the insulin protein,31 a feature which has been used to noncovalently decorate insulin with prosthetic groups for its stable formulation. 32,33 The affinity of CB[7] for Phe in both its amino acid and N-terminal peptide forms, coupled with CB[7] binding to Raman-active NP surfaces, affords several ideal characteristics as a capture-based SERS detection assay for these specific analytes and proteins.

In this paper, we leverage the affinity of CB[7] to increase SERS sensitivity of Phe detection and apply this method to peptides with an N-terminal Phe. Specifically, we demonstrate the ability of CB[7]—Phe complexation to increase the SERS limit of detection (LOD) of Phe. This CB[7]—Phe interaction is further employed to detect larger Phe-terminated peptides such as insulin. The sensitivity advantages of these CB[7]—Phe SERS assays, measured initially on a tabletop instrument, are reproduced using a handheld Raman device, illustrating the ease with which this technology may be deployed as a point-of-care assay. Utilization of CB[7] as a capture agent for Phe and Pheterminated peptides thus provides higher sensitivity in SERS detection with potential applications in the diagnosis and treatment of PKU and diabetes.

Experimental

Materials

I-Adamantylamine (AdNH₂) (Sigma Chemical Co., 98%), L-phenylalanine (Sigma Chemical Co.), glyoxal (Alfa Aesar, 40% w/w aq. Soln), urea (Acros Organics, 99+%), paraformaldehyde (Sigma Aldrich, 95%), sulfuric acid (VWR, 95–98%), Phe-Val, Phe-Val-Asn, and Phe-Val-Asn-Gln peptides (GenScript Inc., ≥95%), HCI (Sigma-Aldrich), and IPA (VWR) were purchased and applied without further purification. Insulin (Recombinant Human Insulin, Gibco) was diluted to I mg/mL using Hank's Buffered Saline Solution (VWR). Ultrapure water (18 M·cm) was obtained from a Millipore Nanopure system (Thermo Fisher Scientific).

CB[7] Synthesis

Briefly, glycoluril monomers were efficiently synthesized in high yield using previously established methods.³⁴ These glycoluril monomers underwent acid-catalyzed polymerization and cyclization to form a mixture of CB[n] species. CB[6] and CB[8] impurities were removed through subsequent rounds of recrystallization in water, yielding purified CB[7]. B35 Purity of CB[7] was verified by hydrogen nuclear magnetic resonance, shown in Figure SI (Supplemental Material). Structures of the glycoluril monomer and CB[7] macrocycle are presented in Fig. Ia.

Preparation of SERS Samples

Ag colloids were prepared using the Lee and Miesel method; 36 91.7 mg of silver nitrate was added to 500 mL of deionized (DI) $\rm H_2O$ and brought to a boil under continuous stirring. Then 10 mL of 38.69 mM sodium citrate was added dropwise and left to stir for 20 min. After cooling to room temperature, colloids were diluted to 1 L with ultrapure water. Transmission electron microscope (TEM) images found in Figure S2a show an average diameter of approximately 40 nm. The colloids were characterized with an ultraviolet–visible (UV–Vis) spectrometer, presented in Figure S2b, showing a $\lambda_{\rm max}$ at 404 nm.

A scheme of the CB[7]–Phe sample preparation can be found in Fig. 1b. CB[7]–Phe and CB[7]–peptide samples for SERS analysis were prepared in 500 μ L of DI H₂O with 7.5 μ L of 10 μ M CB[7], various concentrations of Phe

(aq), and $6\,\mu L$ of 0.25M HCl. The resulting mixture is then vortexed for $60\,\text{min}$ to ensure complete CB[7]—guest encapsulation. One milliliter of Ag colloids was then added to the CB[7]—Phe solution and vortexed for $10\,\text{min}$, resulting in self-aggregation of AgNPs. SERS measurements of aggregated samples were acquired using both the tabletop and handheld setups. All acquired SERS and Raman measurements are non-resonant, as CB[7] and all analytes tested do not have electronic resonances in the visible region.

CB[7]—insulin samples were prepared by functionalizing I mL of AgNP colloids with I μ L of I mM CB[7] and vortexing for 30 min. Insulin was then added to the CB[7] capped AgNPs, and lightly stirred as to avoid aggregation of insulin and allowed to sit for I h. Five microliters of the sample was then dropped onto a clean glass slide and allowed to evaporate, leaving behind an aggregation of AgNPs on the outer edge known as a "coffee ring".

Non-specific binding experiments using AdNH $_2$ and CB[7] in a 1:1 ratio were performed using a similar procedure to the CB[7]–Phe assay. A final concentration of 50 nM AdNH $_2$ and CB[7], with 50 μ M guest, and 6 μ L of 0.25M HCl was prepared in 500 mL of DI H $_2$ O. The mixture was vortexed for 60 min, then I mL of AgNPs was added and vortexed for 10 min, with self-aggregation observed.

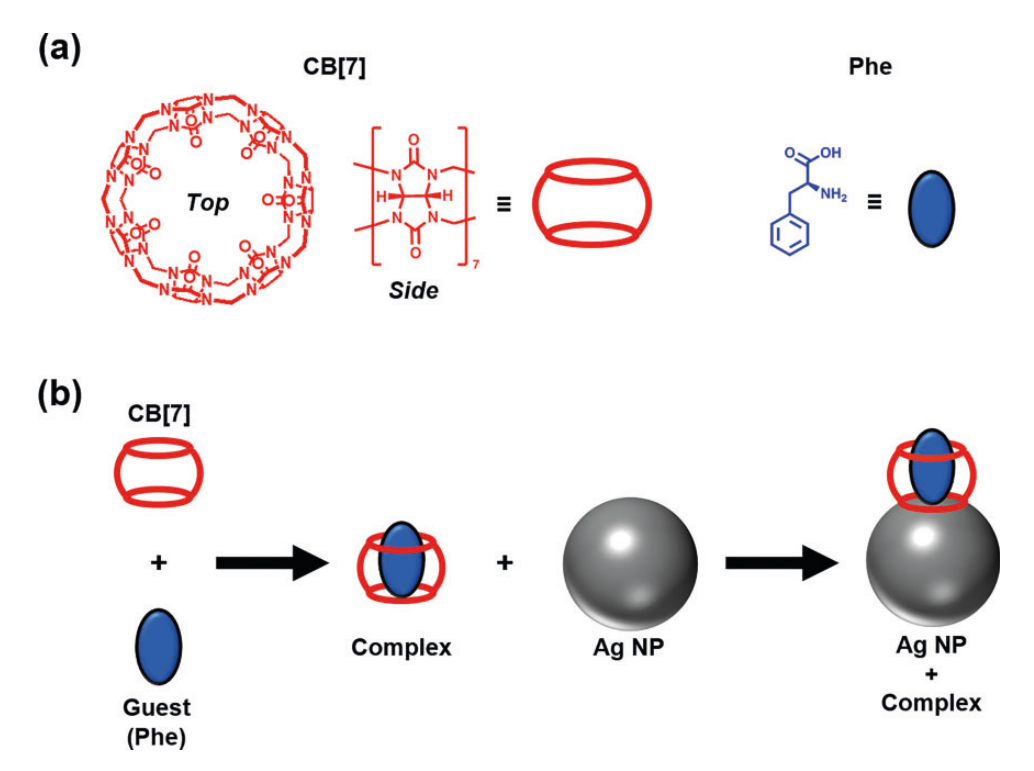


Figure 1. (a) CB[7] macrocycle shown looking down through the cavity in quasi-3D with the C=O rim shown pointing inwards towards the cavity. CB[7] shown as one glycoluril block, and the schematic depiction of CB[7] (left). The molecular structure of Phe and schematic depiction (right). (b) Schematic of the sample preparation. CB[7] and Phe guest are mixed to make the CB[7]—guest complex. The complex is then added to AgNP colloids where the CB[7]—guest complex adsorbs via the carbonyl rim to the surface of the AgNP. Dimensions are not to scale.

SERS Measurements

SERS spectra were acquired using a custom-built setup using a 633 nm HeNe laser (Thor Labs). The laser was focused using an inverted microscope with I mW of power at the objective (Nikon Ti–U, $20\times$, NA = 0.5). Backscattered radiation was then passed through a Rayleigh rejection filter (Semrock) and dispersed with a spectrometer (Princeton Instruments Acton SP2300, f=0.3 mm I200 g/mm). Light was then detected with a back illuminated, deep depletion CCD (PIXIS Spec-I0 Princeton Instruments) and analyzed using Winspec32 software (Princeton Instruments) with a typical integration time of 30 s. All spectra are background subtracted and plotted using IGOR Pro (WaveMetrics).

Portable Raman spectra were obtained using a 785 nm laser powered CBEx system (Snowy Range Instruments) which uses orbital raster scanning to sample a large area. Measurements were taken under 70 mW and 2s of integration time.

Results and Discussion

Phenylalanine

We first determined the Phe SERS LOD using citrate-capped AgNPs as a baseline for the CB[7]–Phe assay. Figure 2a shows 633 nm Raman of Phe, with characteristic peaks at 1004 cm⁻¹ and 1030 cm⁻¹ corresponding to the symmetric ring breathing mode and in-plane ring C–H bending mode, respectively.³⁹ Upon adsorption to AgNPs, the SERS spectra show a similar signature, with a slight shift

in the breathing mode to 1002 cm⁻¹ and the bending mode to 1031 cm⁻¹, consistent with literature.⁴⁰ The following LOD determinations are based on the following equation:

$$LOD = 3\sigma/m \tag{I}$$

where σ is the standard deviation of the blank and m is the slope of the calibration line. For each analyte concentration, three samples were prepared, with each sample measured in triplicate, resulting in nine total spectra which were averaged to produce one SERS spectrum for each sample. In Figs. 2b, 3b, and 4b, the points represent the mean and error bars represent the standard deviation of the mean. For analysis, the Phe peak area of the $1002\,\text{cm}^{-1}$ band was chosen, as it is the most intense in the SERS spectra. Figure 2b displays the $1002\,\text{cm}^{-1}$ peak area as a function of Phe concentration, with the linear response observed in the $400-1200\,\mu\text{M}$ range $(r^2\!=\!0.96)$. SERS of Phe on AgNP aggregates yields an LOD of $35\pm5\,\mu\text{M}$. This value is reasonable compared to studies under similar conditions. $^{16.41}$

Figure I shows a schematic of the CB[7]–guest assay employed for the CB[7]–Phe SERS experiments. Formation of the CB[7]–Phe complex induces changes in the SERS spectra, indicated in Fig. 3a. Characteristic CB[7] SERS bands appear at 444 cm⁻¹, 833 cm⁻¹, and I 190 cm⁻¹, corresponding to the ring scissor mode, ring deformation mode, and a combination C–N stretch and C–H deformation mode, respectively. As Phe threads the CB[7] cavity, the intense Phe breathing mode at I002 cm⁻¹ band shifts slightly in the CB[7]–Phe spectra to I003 cm⁻¹. In order to prove the observed Phe vibrational mode is due

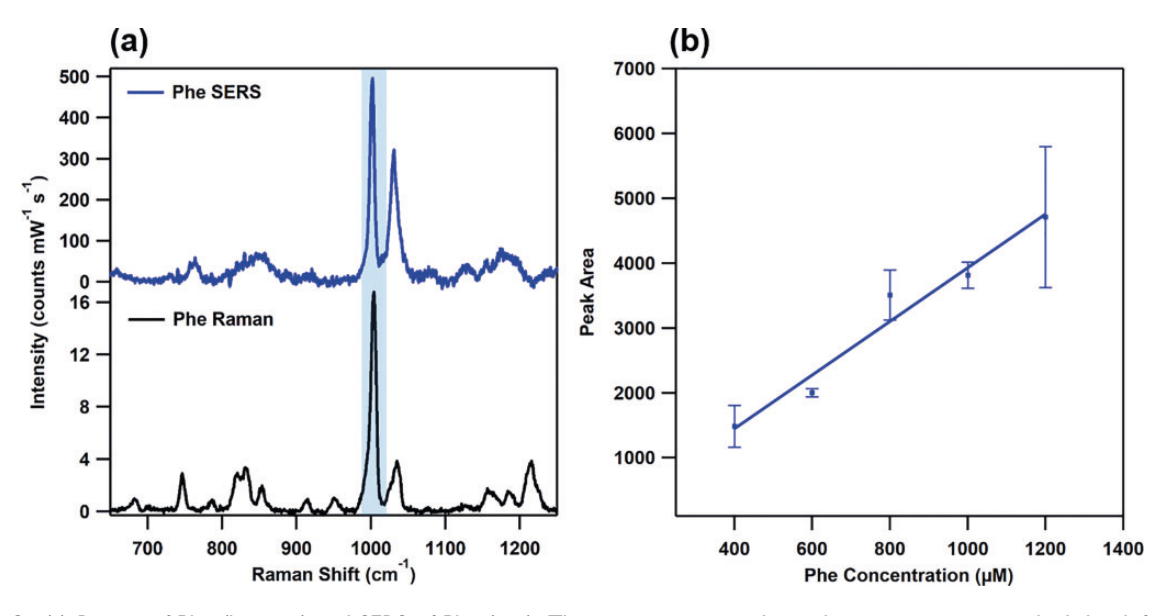


Figure 2. (a) Raman of Phe (bottom) and SERS of Phe (top). The most intense peaks in the spectra persist with slight shifts from Raman to SERS from $1004\,\mathrm{cm^{-1}}$ to $1002\,\mathrm{cm^{-1}}$ and $1030\,\mathrm{cm^{-1}}$ to $1031\,\mathrm{cm^{-1}}$. The highlight indicates the peak used for quantitative analysis. (b) Peak area of the $1002\,\mathrm{cm^{-1}}$ peak versus the Phe concentration (μ M). Each point represents the average peak area ratio of three samples with the error bars representing the standard deviation between samples.

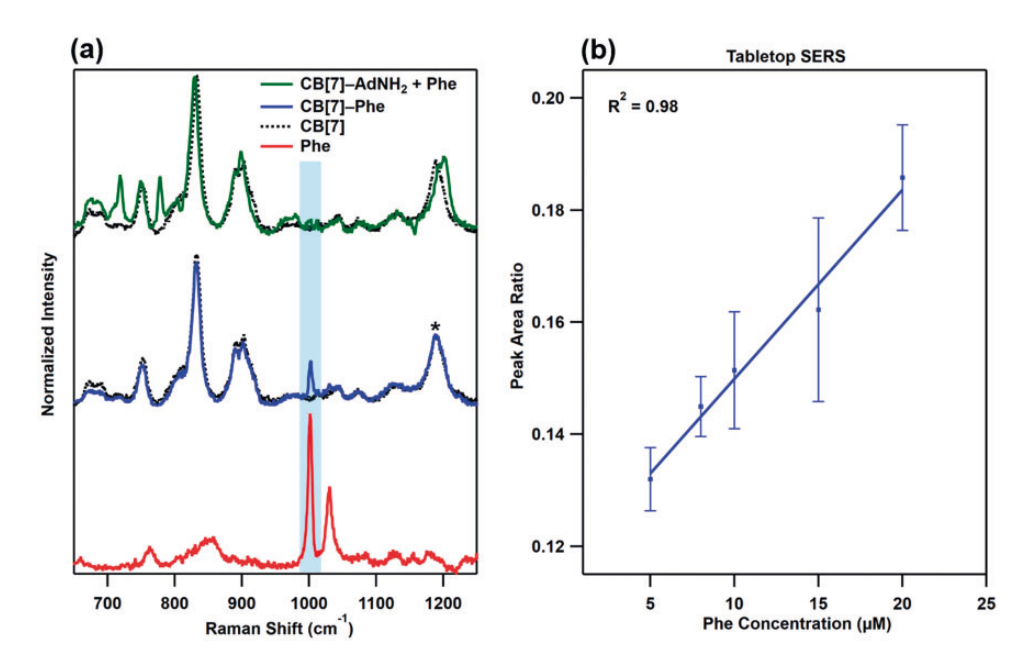


Figure 3. (a) SERS of Phe (bottom), CB[7] (dashed), CB[7]–Phe (middle), and the CB[7]–AdNH₂ with excess Phe (top). Intensities of the CB[7] and CB[7]–Phe are normalized to the constant I I 90 cm⁻¹ mode (*), whereas the rest are normalized to the most intense peak. The appearance of the I 003 cm⁻¹ peak (highlighted) in the CB[7]–Phe spectra indicates the complexation of Phe inside CB[7]. CB[7]–AdNH₂ + Phe shows characteristic AdNH₂ SERS peaks at 720 cm⁻¹ and 779 cm⁻¹. Since no Phe peak at I 003 cm⁻¹ is present, we can attribute the I 003 cm⁻¹ peak in the CB[7]–Phe SERS spectrum to the CB[7]–Phe complex instead of non-specific binding. (b) Peak area ratio of the I 003 cm⁻¹ peak (highlighted) to the I I 90 cm⁻¹ CB[7] peak (*) versus the Phe concentration (μM). Each point represents the average peak area ratio of three samples with the error bars representing the standard deviation between samples.

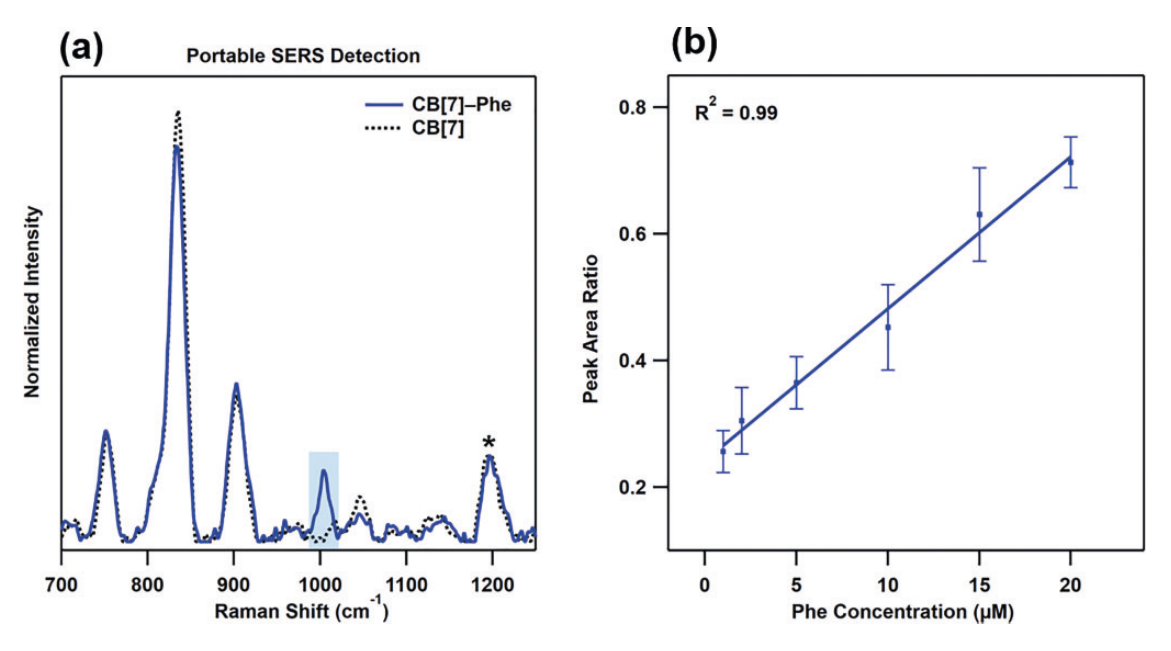


Figure 4. (a) SERS of CB[7] (dashed) and the CB[7]–Phe complex (solid) using the portable Raman spectrometer. Intensities are normalized to the constant 1190 cm $^{-1}$ peak (*). The appearance of the 1003 cm $^{-1}$ peak (highlighted) in the CB[7]–Phe spectra indicates the complexation of Phe inside CB[7]. (b) Peak area ratio of the 1003 cm $^{-1}$ Phe peak to the 1190 cm $^{-1}$ CB[7] peak versus the Phe concentration (μ M). Each point represents the average peak area ratio of three samples with the error bars representing the standard deviation between samples.

to a CB[7]-Phe complex instead of free Phe on the AgNP surface, non-specific binding experiments were performed using a competition-based method with the high affinity guest I-adamantylamine (AdNH₂). AdNH₂ is a 3D cycloalkane compound with a CB[7] K_a on the order of 10^{12} M⁻¹,⁴⁴ many orders of magnitude higher than Phe. For reference, Figure S3 shows SERS spectra of AdNH₂ as well as SERS for the CB[7]-AdNH₂ complex, with characteristic CB[7]-AdNH₂ peaks at 721 cm⁻¹ and 779 cm⁻¹. When AdNH₂ is present with CB[7] and Phe, virtually all CB[7] should be complexed with AdNH₂, and any observed Phe SERS response is due to free Phe bound to the AgNP surface. Figure 3a shows the CB[7]-AdNH₂ signature while the Phe peak is absent. Based on these experiments, we can attribute the observed SERS response to a CB[7]-Phe complex on the AgNP surface.

The presence of sodium cations and alterations in pH are known environmental mediators of CB[7] amino acid affinity. Previous studies of CB[7]-amino acid interactions in aqueous solutions have determined that CB[7]-Phe binding is optimal at pH7 or lower, where the amine and carboxylate groups are protonated, thus fostering ion-dipole interactions with the CB[7] carbonyls.²⁸ Also, Na⁺ has been shown to decrease CB[7]-Phe binding affinities due to its competitive complexation with the carbonyl portals. 28,45 In our sample of AgNPs with CB[7] and Phe, the pH is 8 and NaBr must be added in order to induce aggregation. Samples prepared in the native pH with NaBr show no SERS evidence of the CB[7]-Phe interaction. To avoid Na⁺ interference and induce AgNP aggregation, the solution is acidified to pH 6 with HCl, and evidence of the characteristic Phe 1003 cm⁻¹ mode appears.

Quantitative SERS measurements of the CB[7]-Phe complex were performed in order to determine the advantage in SERS sensitivity of CB[7]-guest interaction. In order to improve accuracy, a ratiometric peak area ratio was employed, as it has been previously shown to reduce signal fluctuations while maintaining sensitivity among SERS methods. 13,15,46 Across all concentrations of Phe, the 1190 cm⁻¹ CB[7] band, which is not attributed to a ring deformation, was used as a reference peak.⁴² This peak exhibited less fluctuations (\sim 5% standard deviation in the peak area) compared to the ring breathing modes (15% standard deviation in the peak area). Figure 3b plots the Phe to CB[7] peak area ratio as a function of Phe concentration in the linear range of $5-20 \,\mu\text{M}$ ($r^2=0.98$). An expanded concentration range (Figure S4) shows an equilibrium in CB[7]-Phe binding around 30 μM. This host-guest assay yields an LOD of $7.3 \pm 1.8 \,\mu\text{M}$, providing a $\sim \! 5 \times \text{greater LOD}$ than for the Phe guest alone. While we do not attempt to quantify the enhancement factor in this work, this result makes sense, as CB[7] has been proven to increase SERS enhancements by many orders of magnitude through forming well-defined hotspots.²¹ These results show the advantage in SERS sensitivity offered by CB[7]-Phe complexation.

This host-guest assay can be easily applied to portable detection through use of a handheld Raman spectrometer. The CB[7]-Phe assay had similar results to the custom-built tabletop setup, as seen in Figure 4, with a linear response in the 5–30 μM range. LOD calculations gave a Phe LOD of $79 \pm 12 \,\mu\text{M}$, and a CB[7]–Phe LOD of $3.0 \pm 0.7 \,\mu\text{M}$, representing a \sim 25 \times improvement in LOD by CB[7] capture. In this case, the portable Raman system provides a slightly higher LOD than the tabletop setup for the detection of Phe alone. This is likely due to the larger sampling area and high resolution afforded by the raster scanning abilities of the portable system. The ability to analyze a similar concentration range as the tabletop setup shows the CB[7]-Phe system is largely unaffected by the higher wavelength laser and lower grating resolution afforded by the portable instrumentation. The use of a cost-effective portable instrumentation establishes the applicability of this assay in field settings at a relatively inexpensive price.

Phenylalanine-Terminated Peptides

For larger biomolecules, SERS characterization can become more challenging, as the variety of functional groups can lead to multiple binding geometries and low surface affinity. This leads to broadened peaks, inconsistent SERS responses, and inconsistent aggregation effects.⁴⁷ In an attempt to account for the increased steric bulk of insulin, the first three peptides of the N-terminal B-chain sequence of insulin were tested with the CB[7] SERS assay. The peptides tested, presented in Fig. 5, are the successive additions of the first four amino acid residues in the sequence: Phe, valine (Val), asparagine (Asn), and glutamine (Gln). Namely, Phe-Val (P1), Phe-Val-Asn (P2), and Phe-Val-Asn-Gln (P3). Raman and SERS of these compounds, seen in Figure S5, show peaks attributed to the Phe residue at 1003 cm⁻¹ and 1032 cm⁻¹, consistent with previous observations.⁴⁸ To determine the effect of additional amino acid residues on the CB[7]-Phe interaction, the peptides were tested using the same procedure as in the CB[7]-Phe experiments. Upon CB[7] complexation with the PI peptide, the $1003 \, \text{cm}^{-1}$ mode in the SERS spectra persists, as seen in Fig. 5, confirming threading of the Phe residue inside the CB[7] cavity. This response was also observed for peptides P2 and P3, an indication that CB[7]-Phe complexation is unhindered by the additional amino acid residues. This result aligns with a previous study on the CB[7] interaction with the B chain of insulin, in which the Val and Asn contribute to stabilization of the interaction.31 To further confirm the CB[7]-peptide interaction on the surface, nonspecific binding experiments were performed with AdNH₂ as the competitive guest. SERS spectra found in Figure S6 indicate presence of the CB[7]-AdNH2 complex on the surface, with the 721 cm⁻¹ and 779 cm⁻¹ peaks and no presence of the 1003 cm⁻¹ Phe mode, indicating a negligible contribution of non-specific binding. Observation of the

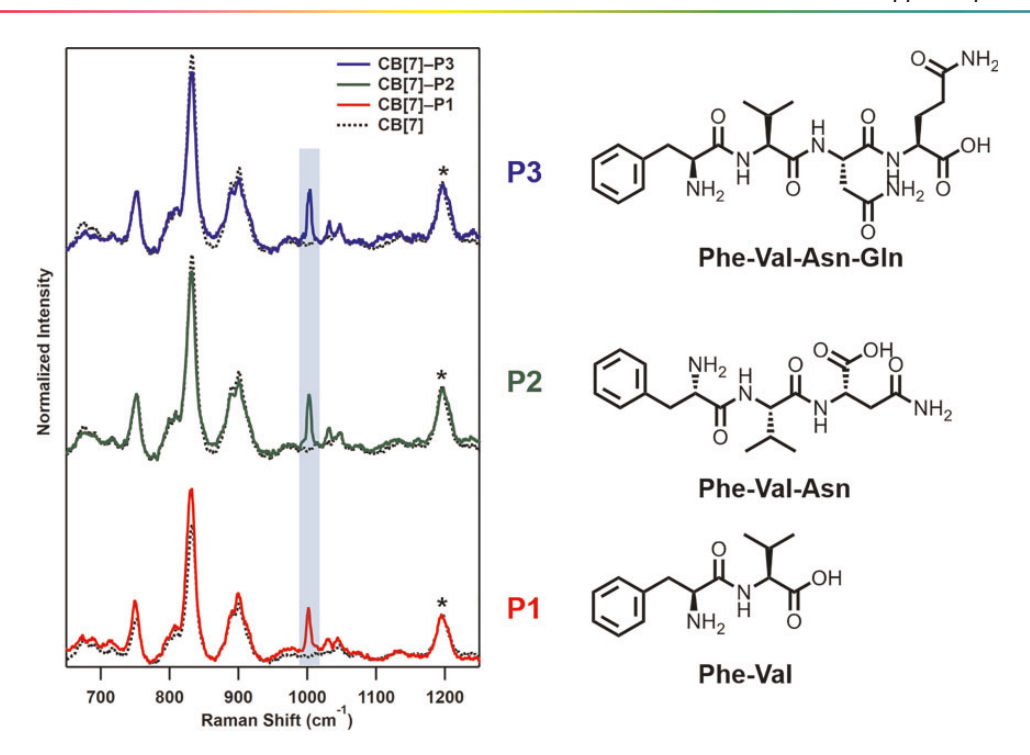


Figure 5. SERS of CB[7]—peptide complexes and the primary sequence of each peptide from the insulin *N*-terminus of the B-chain peptide chain. CB[7] (dashed), CB[7]—P1 (bottom), CB[7]—P2 (middle), and CB[7]—P3 (top). Intensities of all spectra are normalized to the constant 1190 cm⁻¹ mode (*). The appearance of the 1003 cm⁻¹ peak (highlighted) in the spectra indicates the CB[7]—peptide complexation through the Phe residue.

1003 cm⁻¹ Phe mode in the CB[7] complex with Phe-terminal peptides confirms the CB[7]–Phe SERS assay can be easily applied to larger peptides.

Insulin

The SERS of a CB[7]-insulin complex was measured in order to determine if the CB[7]-Phe assay can be extended into larger Phe-terminated proteins with relevance in point-ofcare detection. SERS of larger macromolecules has proven difficult as NP-analyte localization is hampered due to sterics and lower surface affinity. A facile method to overcome this issue is the widely used drop-cast method, 49,50 which has been previously used for CB[7]-guest systems.⁵¹ The drop-cast method is shown in Fig. 6a, where AgNP colloids mixed with an analyte are dropped onto a glass slide and, as the drop evaporates, the functionalized NPs are concentrated at the edge of the drop, forming a coffee ring. SERS of insulin on AgNPs using the drop-cast method, seen in Fig. 6b, shows an intense peak at 1002 cm⁻¹ attributed to the Phe residue at the N-terminus, as expected. 52,53 To validate the use of CB[7]-functionalized AgNPs as a viable method for CB[7]-Phe complexation and detection with the drop-cast method, Phe itself was first tested. SERS spectra of the CB[7]-Phe complex can be found in Figure S7, where spectra are consistent with the AgNP solution-phase aggregation method, indicating this method accurately induces a CB[7]-Phe interaction on the surface that can be measured

with SERS. When applied to insulin, SERS of the CB[7]-insulin complex follow the same trend as the CB[7]-Phe characteristic peaks, where a Phe peak slightly shifted to 1003 cm⁻¹ appears, indicative of CB[7]-insulin binding through the Phe residue, as seen in Fig. 6b. To ensure the SERS spectrum is showing a CB[7]-insulin complex, nonspecific binding experiments using the competitive guest AdNH₂ were performed. Figure 6b shows that when insulin and AdNH₂ are introduced to CB[7] functionalized AgNPs, the characteristic CB[7]-AdNH₂ SERS peaks appear with no 1003 cm⁻¹ Phe peak present. From this result we can attribute the 1003 cm⁻¹ peak to the Phe residue on the B-chain of the insulin complexed with the AgNP surface-bound CB[7]. The CB[7]-Phe interaction provides a consistent surface interaction and characterization through the Phe mode even for a larger peptide consisting of 51 amino acids. Further, equilibrium binding affinity between CB[7] and guest molecules has been observed to decrease when transitioning from pure water to culture medium with 10% Fetal Bovine Serum. 45 This interference arises from the presence of sodium salts and soluble amino acids, such as Phe. However, N-terminal Phe has been shown to outcompete both mid-chain and monomer aromatic amino acids due to the CB[7] carbonyl portal coordinating the N-terminal ammonium group, 31 which should still provide selectivity for insulin binding in biological samples. 29,30 The ability to detect a larger Phe-terminated peptide through CB[7]-Phe binding displays the utility of this host-guest assay to enable

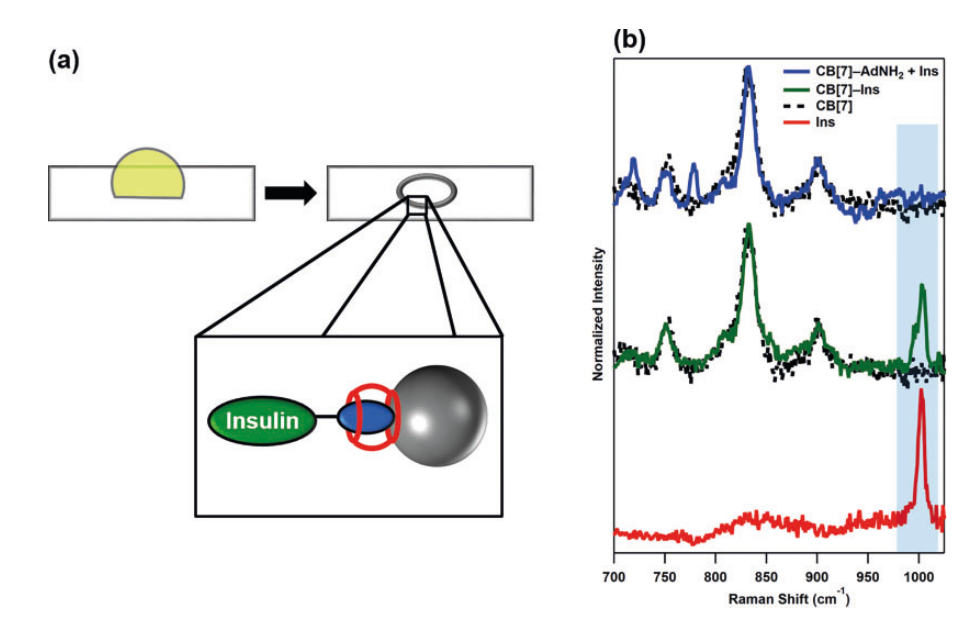


Figure 6. (a) Schematic of the drop-cast method. The yellowish-green hemisphere is a drop of the Ag colloid functionalized with CB[7]—guest on a glass slide. The drop then evaporates and leaves a coffee ring of the functionalized AgNPs. The black box indicates a zoom in on the coffee ring aggregation, with a cartoon of the CB[7]—insulin host—guest complex binding through the Phe residue. (b) SERS of insulin (Ins) (bottom), CB[7] (dashed), CB[7]—Ins (middle), and CB[7]—AdNH₂ with excess insulin (top). Intensities are normalized to the 833 cm⁻¹ mode. Insulin shows a characteristic peak from Phe at 1002 cm⁻¹ (highlighted). The CB[7]—Ins spectrum shows the Phe peak persists with a slight shift to 1003 cm⁻¹. The non-specific binding experiment with AdNH₂ shows no SERS peak attributable to non-specific binding of insulin.

detection of larger peptides and proteins with clinical relevance.

Conclusion

We present an analytical SERS assay for detection of Phe and Phe-terminated peptides through complexation with the CB[7] macrocycle. The CB[7]-Phe assay shows improvements in SERS sensitivity on tabletop and portable Raman setups with $5 \times \text{and } 25 \times \text{lower LODs}$, respectively. This assay's utility to detect biologically relevant molecules is shown by applying the CB[7]-Phe assay to Phe-terminated peptides found in the B-chain of insulin as well as to insulin itself. Further optimization of this method could lead to selective quantification of insulin through CB[7]-Phe residue interaction for clinical diagnosis/treatment of diabetes. This method could also be extended to the vast library of metabolites, especially those with N-terminal aromatic groups, for increased sensitivity of SERS detection.⁵⁴ These results show that through simple sample preparation of CB[7]-functionalized silver nanoparticles, quantitative SERS detection can be significantly improved and scaled to larger, clinically relevant proteins.

Declaration of Conflicting Interests

The author(s) declared no potential conflicts of interest with respect to the research, authorship, and/or publication of this article.

Funding

This material is based upon work supported by the National Science Foundation under grant numbers CHE_1709566 (J.E.O. and J.P.C.). Any opinions, findings, and conclusions or recommendations expressed in this material are those of the authors and do not necessarily reflect the views of the National Science Foundation. Support from the American Diabetes Association is also appreciated (I_19_ACE_31, M.J.W.). Additionally, we acknowledge support from a Seed Grant through Notre Dame Nanoscience and Technology (NDnano, J.P.C. and M.J.W.). This work was also supported by the University of Notre Dame (all authors).

ORCID iDs

Supplemental material

The supplemental material mentioned in the text, consisting of eight figures, is available in the online version of the journal.

References

- C.R. Scriver, P.J. Waters, C. Sarkissian, et al. "PAHdb: A Locus-Specific Knowledgebase". Hum. Mutat. 2000. 15(1): 99–104.
- N. Blau, FJ. van Spronsen, H.L. Levy. "Phenylketonuria". Lancet. 2010. 376(9750): 1417–1427.
- C.O. Gregory, C. Yu, R.H. Singh. "Blood Phenylalanine Monitoring for Dietary Compliance among Patients with Phenylketonuria: Comparison of Methods". Genet. Med. 2007. 9(11): 761–765.

- K.M. Cheung, K.-A. Yang, N. Nakatsuka, et al. "Phenylalanine Monitoring Via Aptamer-Field-Effect Transistor Sensors". ACS Sens. 2019. 4(12): 3308–3317.
- E. Omidinia, N. Shadjou, M. Hasanzadeh. "Aptamer-Based Biosensor for Detection of Phenylalanine at Physiological pH". Appl. Biochem. Biotechnol. 2014. 172(4): 2070–2080.
- Y. Shen, W. Prinyawiwatkul, Z. Xu. "Insulin: A Review of Analytical Methods". Analyst. 2019. 144(14): 4139–4148.
- X. Zhang, S. Zhu, C. Deng, et al. "An Aptamer Based On-Plate Microarray for High-Throughput Insulin Detection by MALDI-TOF MS". Chem. Commun. 2012. 48(21): 2689–2691.
- M. Frasconi, C. Tortolini, F. Botre, et al. "Multifunctional Au Nanoparticle Dendrimer-Based Surface Plasmon Resonance Biosensor and Its Application for Improved Insulin Detection". Anal. Chem. 2010. 82(17): 7335–7342.
- Y. Wang, D. Gao, P. Zhang, et al. "A Near Infrared Fluorescence Resonance Energy Transfer Based Aptamer Biosensor for Insulin Detection in Human Plasma". Chem. Commun. 2014. 50(7): 811–813.
- J. Langer, D. Jimenez de Aberasturi, J. Aizpurua, et al. "Present and Future of Surface-Enhanced Raman Scattering". ACS Nano. 2020. 14(1): 28–117.
- S.-Y. Ding, E.-M. You, Z.-Q. Tian, et al. "Electromagnetic Theories of Surface-Enhanced Raman Spectroscopy". Chem. Soc. Rev. 2017. 46(13): 4042–4076.
- C. Murray, D. Allara, M. Rhinewine. "Silver-Molecule Separation Dependence of Surface-Enhanced Raman Scattering". Phys. Rev. Lett. 1980. 46(1): 57.
- X. Gu, J.P. Camden. "Surface-Enhanced Raman Spectroscopy-Based Approach for Ultrasensitive and Selective Detection of Hydrazine". Anal. Chem. 2015. 87(13): 6460–6464.
- 14. X. Gu, M.J. Trujillo, J.E. Olson, et al. "SERS Sensors: Recent Developments and a Generalized Classification Scheme Based on the Signal Origin". Annu. Rev. Anal. Chem. 2018. 11(1): 147–169.
- M.J. Trujillo, D.M. Jenkins, J.A. Bradshaw, et al. "Surface-Enhanced Raman Scattering of Uranyl in Aqueous Samples: Implications for Nuclear Forensics and Groundwater Testing". Anal. Methods. 2017. 9(10): 1575–1579.
- 16. B. Murugesan, J. Yang. "Tunable Coffee Ring Formation on Polycarbonate Nanofiber Film for Sensitive SERS Detection of Phenylalanine in Urine". ACS Omega. 2019. 4(12): 14928–14936.
- B. Fazio, C. D'Andrea, A. Foti, et al. "SERS Detection of Biomolecules at Physiological Ph Via Aggregation of Gold Nanorods Mediated by Optical Forces and Plasmonic Heating". Sci. Rep. 2016. 6(1): 26952.
- J. Kim, I.-S. Jung, S.-Y. Kim, et al. "New Cucurbituril Homologues: Syntheses, Isolation, Characterization, and X-ray Crystal Structures of Cucurbit [N] Uril (N = 5, 7, and 8)". J. Am. Chem. Soc. 2000. 122(3): 540–541.
- A.S. Braegelman, M.J. Webber. "Integrating Stimuli-Responsive Properties in Host-Guest Supramolecular Drug Delivery Systems". Theranostics. 2019. 9(11): 3017.
- S. Sinn, F. Biedermann. "Chemical Sensors Based on Cucurbit [N]Uril Macrocycles". Isr. J. Chem. 2018. 58(3–4): 357–412.
- C.-A. Tao, Q. An, W. Zhu, et al. "Cucurbit[N]Urils as a SERS Hot-Spot Nanocontainer through Bridging Gold Nanoparticles". Chem. Commun. 2010. 47(35): 9867–9869.
- S. Kasera, F. Biedermann, J.J. Baumberg, et al. "Quantitative SERS Using the Sequestration of Small Molecules inside Precise Plasmonic Nanoconstructs". Nano Lett. 2012. 12(11): 5924–5928.
- D.O. Sigle, S. Kasera, L.O. Herrmann, et al. "Observing Single Molecules Complexing with Cucurbit[7]Uril Through Nanogap Surface-Enhanced Raman Spectroscopy". J. Phys. Chem. Lett. 2016. 7(4): 704–710.
- B. de Nijs, M. Kamp, I. Szabó, et al. "Smart Supramolecular Sensing with Cucurbit[N]Urils: Probing Hydrogen Bonding with SERS". Faraday Discuss. 2017. 205: 505–515.

- S.J. Barrow, S. Kasera, M.J. Rowland, et al. "Cucurbituril-Based Molecular Recognition". Chem. Rev. 2015. 115(22): 12320–12406.
- L. Cao, M. Šekutor, P.Y. Zavalij, et al. "Cucurbit [7]Uril Guest Pair with an Attomolar Dissociation Constant". Angew. Chem. Int. Ed. 2014. 53(4): 988–993.
- W.S. Jeon, K. Moon, S.H. Park, et al. "Complexation of Ferrocene Derivatives by the Cucurbit[7]Uril Host: A Comparative Study of the Cucurbituril and Cyclodextrin Host Families". J. Am. Chem. Soc. 2005. 127(37): 12984–12989.
- J.W. Lee, H.H.L. Lee, Y.H. Ko, et al. "Deciphering the Specific High-Affinity Binding of Cucurbit[7]Uril to Amino Acids in Water". J. Phys. Chem. B. 2015. 119(13): 4628–4636.
- J.W. Lee, M.H. Shin, W. Mobley, et al. "Supramolecular Enhancement of Protein Analysis Via the Recognition of Phenylalanine with Cucurbit[7]Uril". J. Am. Chem. Soc. 2015. 137(48): 15322–15329.
- A.R. Urbach, V. Ramalingam. "Molecular Recognition of Amino Acids, Peptides, and Proteins by Cucurbit [N] Uril Receptors". Isr. J. Chem. 2010. 51(5–6): 664–678.
- J.M. Chinai, A.B. Taylor, L.M. Ryno, et al. "Molecular Recognition of Insulin by a Synthetic Receptor". J. Am. Chem. Soc. 2010. 133(23): 8810–8813.
- C.L. Maikawa, A.A. Smith, L. Zou, et al. "Stable Monomeric Insulin Formulations Enabled by Supramolecular Pegylation of Insulin Analogues". Adv. Ther. 2019. 3(1): 1900094.
- M.J. Webber, E.A. Appel, B. Vinciguerra, et al. "Supramolecular Pegylation of Biopharmaceuticals". Proc. Natl. Acad. Sci. U.S.A. 2016. 113(50): 14189–14194.
- L.A. Wingard, E.C. Johnson, J.J. Sabatini. "Efficient Method for the Cycloaminomethylation of Glycoluril". Tetrahedron Lett. 2016. 57(15): 1681–1682.
- D. Jiao, N. Zhao, O.A. Scherman. "A 'Green' Method for Isolation of Cucurbit [7]Uril via a Solid-State Metathesis Reaction". Chem. Commun. 2010. 46(12): 2007–2009.
- P. Lee, D. Meisel. "Adsorption and Surface-Enhanced Raman of Dyes on Silver and Gold Sols". J. Phys. Chem. 1982. 86(17): 3391–3395.
- E.A. Appel, F. Biedermann, D. Hoogland, et al. "Decoupled Associative and Dissociative Processes in Strong yet Highly Dynamic Host–Guest Complexes". J. Am. Chem. Soc. 2017. 139(37): 12985–12993.
- L. Zou, A.S. Braegelman, M.J. Webber. "Dynamic Supramolecular Hydrogels Spanning an Unprecedented Range of Host–Guest Affinity". ACS Appl. Mater. Interfaces. 2019. 11(6): 5695–5700.
- F. Wei, D. Zhang, N.J. Halas, et al. "Aromatic Amino Acids Providing Characteristic Motifs in the Raman and SERS Spectroscopy of Peptides". J. Phys. Chem. B. 2008. 112(30): 9158–9164.
- S.K. Kim, M.S. Kim, S.W. Suh. "Surface-Enhanced Raman Scattering (SERS) of Aromatic Amino Acids and their Glycyl Dipeptides in Silver Sol". J. Raman Spectrosc. 1987. 18(3): 171–175.
- R.B. Jeffers, J.B. Cooper. "FT-Surface-Enhanced Raman Scattering of Phenylalanine Using Silver-Coated Glass Fiber Filters". Spectrosc. Lett. 2010. 43(3): 220–225.
- M.L. Roldán, S. Sanchez-Cortes, J.V. García-Ramos, et al. "Cucurbit [8] Uril-Stabilized Charge Transfer Complexes with Diquat Driven by pH: A SERS Study". Phys. Chem. Chem. Phys. 2012. 14(14): 4935–4941.
- S. Mahajan, T.-C. Lee, F. Biedermann, et al. "Raman and SERS Spectroscopy of Cucurbit[N]Urils". Phys. Chem. Chem. Phys. 2010. 12(35): 10429–10433.
- S. Liu, C. Ruspic, P. Mukhopadhyay, et al. "The Cucurbit[N]Uril Family: Prime Components for Self-Sorting Systems". J. Am. Chem. Soc. 2005. 127(45): 15959–15967.
- H. Wu, H. Chen, B. Tang, et al. "Host–Guest Interactions between Oxaliplatin and Cucurbit[7]Uril/Cucurbit[7]Uril Derivatives Under Pseudo-Physiological Conditions". Langmuir. 2020. 36(5): 1235–1240.
- R.L. McCreery. Raman Spectroscopy for Chemical Analysis. New York: John Wiley and Sons, 2005.
- 47. I. Bruzas, W. Lum, Z. Gorunmez, et al. "Advances in Surface-Enhanced Raman Spectroscopy (SERS) Substrates for Lipid and Protein

- Characterization: Sensing and Beyond". Analyst. 2018. 143(17): 3990–4008.
- G. Chumanov, R. Efremov, I. Nabiev. "Surface-Enhanced Raman Spectroscopy of Biomolecules. Part I: Water-Soluble Proteins, Dipeptides, and Amino Acids". J. Raman Spectrosc. 1990. 21(1): 43–48.
- M. Banchelli, M. de Angelis, C. D'Andrea, et al. "Triggering Molecular Assembly at the Mesoscale for Advanced Raman Detection of Proteins in Liquid". Sci. Rep. 2018. 8(1): 1033.
- W. Wang, Y. Yin, Z. Tan, et al. "Coffee-Ring Effect-Based Simultaneous SERS Substrate Fabrication and Analyte Enrichment for Trace Analysis". Nanoscale. 2014. 6(16): 9588–9593.
- W.-I.K. Chio, W.J. Peveler, K.I. Assaf, et al. "Selective Detection of Nitroexplosives Using Molecular Recognition within Self-Assembled Plasmonic Nanojunctions". J. Phys. Chem. C. 2019. 123(25): 15769–15776.
- H. Cho, S. Kumar, D. Yang, et al. "Surface-Enhanced Raman Spectroscopy-Based Label-Free Insulin Detection at Physiological Concentrations for Analysis of Islet Performance". ACS Sens. 2018. 3(1): 65–71.
- 53. V. Drachev, M. Thoreson, E. Khaliullin, et al. "Semicontinuous Silver Films for Protein Sensing with SERS". Proc. SPIE. 2003. 5221.
- L.M. Sherman, A.P. Petrov, L.F.P. Karger, et al. "A Surface-Enhanced Raman Spectroscopy Database of 63 Metabolites". Talanta. 2020. 210: 120645.